Reducing Migration of Knee Exoskeletons With Dynamic Waist Strap

Ming Xu, Zhihao Zhou, *Member, IEEE*, Jinyan Shao, Lecheng Ruan, and Qining Wang, *Senior Member, IEEE*

Abstract—Downward migration of knee exoskeletons under external forces is one major concern against their normal operations. It may be reduced by increasing the friction between exoskeletons and the human thigh. However, the effectiveness of friction control remains questionable, as the natural inverted-cone shape of the human thigh will aggravate downward migration, and the overwhelming strapping intensity will degrade the activation level of muscles. In this paper, we propose a new suspension system called the Dynamic Waist Strap. Theoretical analysis and experimental validations on multiple subjects are conducted to show its advantages over the three mainstream suspension systems commonly used for knee exoskeletons in terms of the reduction of migration, interaction torque, and maximum dip angle. This study highlights the importance of the suspension system when attaching a knee exoskeleton to the human and introduces a new dynamic interaction interface to improve the coupling from a knee exoskeleton to an individual.

Index Terms—Knee exoskeleton, migration, thigh cuff, dynamic waist strap.

Ming Xu and Jinyan Shao are with the Department of Advanced Manufacturing and Robotics, College of Engineering and the Institute for Artificial Intelligence, Peking University, Beijing 100871, China, and also with the Beijing Engineering Research Center of Intelligent Rehabilitation Engineering, Beijing 100871, China.

Zhihao Zhou is with the School of Artificial Intelligence and the Department of Advanced Manufacturing and Robotics, College of Engineering, Peking University, Beijing 100871, China.

Lecheng Ruan is with the Beijing Institute for General Artificial Intelligence, Beijing 100080, China, and also with the Department of Advanced Manufacturing and Robotics, College of Engineering, Peking University, Beijing 100871, China.

Qining Wang is with the Department of Advanced Manufacturing and Robotics, College of Engineering, and the Institute for Artificial Intelligence, Peking University, Beijing 100871, China, also with the University of Health and Rehabilitation Sciences, Qingdao 266071, China, and also with the Beijing Institute for General Artificial Intelligence, Beijing 100080, China (e-mail: qiningwang@pku.edu.cn).

I. INTRODUCTION

KNEE extensors play an important role in human bipedal walking [1]. In daily activities, knee extension assistance is meaningful in reducing the fatigue of muscles and the payload of the knee joint due to long-term walking under body weight and external load. Moreover, for patients with neuromuscular disorders, applying knee extension assistance may help them accomplish basic activities regarding independent mobility. Hence, robotic exoskeletons for knee extension assistance have attracted increasing interest over the past decades [2]–[4]. These knee exoskeletons can be divided into two categories according to their main structures: exoskeletons with rigid links and simplified joints, and soft exosuits using textile structures [5]. However, both rigid and soft knee exoskeletons face the same challenge that they suffer from downward migration along the thigh axis when providing assistance, due to the existence of external downward forces [6].

Rotation of the human knee joint is complicated, as the center of rotation (CoR) changes regularly. Rigid exoskeletons adapt to this change with specific mechanisms, resulting in the increases in weight and inertia [10], [11]. For these exoskeletons, the external downward force on the thigh cuff is mainly gravity. The downward migration deteriorates after worn, leading to misalignment and energy dissipation [12], [13]. The soft exosuits, on the other hand, have no rigid frame. They use Bowden cable transmission and textile-based wearable suits to transmit power from actuator to musculoskeletal structure of the human body [14], thus are often lightweight and compact [15]. However, without inflexible structures to absorb or transfer shear forces generated by the human body, soft exosuits are supposed to provide higher assistance magnitude [16]. Then the thigh cuff should resist higher downward force generated by the sheath of the Bowden cable. As a result, the upper cuff of soft exosuits tends to migrate when providing assistance, leading to a leap in the distance between two anchors of Bowden cable, which is not desired for robust control [17].

Therefore, it is important to properly design the physical human-robot interface between knee exoskeletons and the human thigh for reducing migration. The high-tighten-able thigh cuffs (for instance: hook and loop straps [18]–[20], pneumatic cuffs [6], [21] and BOA straps [22]) are designed to solve this problem. However, tightening the thigh cuff to decrease downward drift is not always effective, especially when the external downward force is large. And tightening the

upper cuff could limit the activation of muscles in the human thigh, leading to discomfort or even pain [23], [24]. Other designs employ articular ankle/hip joints [25]–[29] to support the knee exoskeleton. However, the articular ankle/hip joints may hinder the natural motions of the wearer.

To address these problems, several solutions have been proposed. These studies employ the additional webbing strap(s) anchored on a waist belt (as a suspension system) to pull upwards the thigh cuff of knee exoskeletons since the waist belt itself is resistant to downward migration as it can anchor onto the bony landmarks of pelvis [30]. The major difference among these works is how many additional webbing straps are utilized and where webbing straps are arranged. For instance, Evelyn *et al.* routed an additional webbing strap along the lateral side of the hip [16], as shown in Fig. 1(a). Another possible solution (see Fig. 1(b)) placed a zonary structure along the anterior side of the hip [31]–[33], while [31] applied a non-stretchable Nylon webbing belt and [32], [33] employed a tensile rubber band (applied in the Myosuit). In addition, Zhang *et al.* utilized two webbing straps arranged along both the anterior and posterior side of the hip [34] (see Fig. 1(c)). However, in these designs, the webbing strap(s) may be slack or tightened excessively when the hip rotates, since the distance between the waist belt and the thigh cuff changes along with hip rotation, and accomplishing length compensation through deformation may be not reliable.

In this paper, we propose a novel suspension system called the Dynamic Waist Strap. And evaluation methods concerning migration and wearing comfort when utilizing suspension systems are presented. The proposed design does not employ any webbing strap but a wire loop to pull upwards the thigh cuff of knee exoskeletons. Starting from our preliminary study [35], here we evaluated the effectiveness of the proposed Dynamic Waist Strap in an actual scenario. The main contributions of this study can be listed as follows: 1) A novel suspension system is proposed for reducing the migration of knee exoskeletons through dynamic length compensation; 2) An evaluation system is presented to appraise the effects of suspension systems on the human-exoskeleton system quantitatively; 3) The effectiveness of suspension systems commonly used for knee exoskeletons is analyzed in detail.

The rest of this paper is organized as follows. The design and theoretical analysis of the Dynamic Waist Strap are shown in Section II. The experimental setup and protocols are presented in Section III. Section IV shows the experimental results. We discuss and conclude in Section V and Section VI respectively.

II. DYNAMIC WAIST STRAP

A. System Design

A suspension scheme based on dynamic length compensation is proposed since the suspension through the deformation of the webbing strap is not reliable. In this scheme, a dynamic rope loop is employed to pull the thigh cuff upwards from both the front and the back sides. The rope loop can slide along the waist belt during hip flexion/extension to dynamically compensate for the varying length and force requirements for
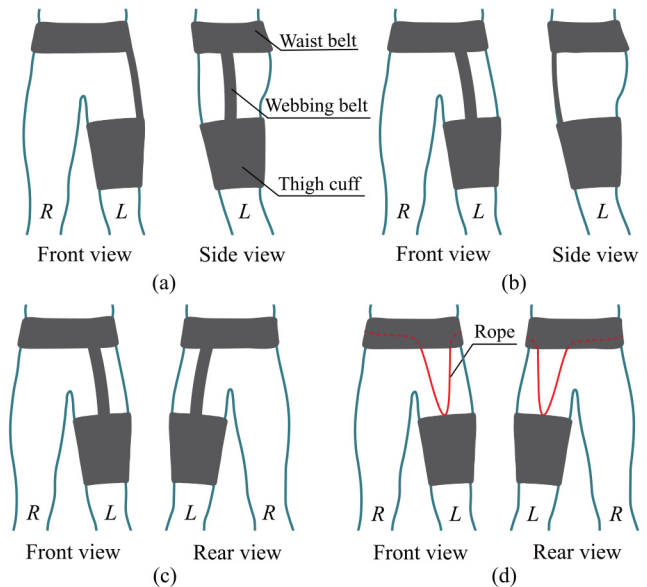

Fig. 1. The suspension schemes for reducing migration of knee exoskeletons. (a) Condition 1 (*C1*): the lateral suspension system proposed in [16], which employed a lateral webbing belt between the waistbelt and the thigh cuff. (b) Condition 2 (*C2*): the frontal suspension system illustrated in [32], [33], which pathed a zonary structure along the anterior side of the hip. (c) Condition 3 (*C3*): the anterior and posterior suspension system demonstrated in [34], which utilized two webbing straps arranged along both the anterior and posterior side of the hip. (d) Condition 4 (*C4*): a probable better idea for dealing with this problem discussed in this paper.

suspension in different hip angles, as shown in Fig. 1(d). Based on this schematic, an anti-skid device named the Dynamic Waist Strap is designed (see Fig. 2). In this design, the rope loop is replaced by a wire loop for the consideration of capability. Several sections of the outer sheath surrounding the wire are embedded in a waist belt to reduce friction when the wire loop slides relative to the waist belt. On the anterior side of the human thigh, the wire loop stretches out from the sheaths and holds the upper front edge of the thigh cuff, when it pulls the upper back edge of the thigh cuff in the back at the same time. The perimeter of the wire loop remains unchanged during the operation, as shown in Fig. 2(d), denoted as $L_f + L_b = $ Constant. During hip flexion, the distance between the front anchor and the waist belt will shorten, and the distance between the back anchor and the waist belt will elongate, and the wire segment in L_f will transmit to L_b accordingly to guarantee that the natural motion of the human hip is not restricted, as depicted in Fig. 2(e). During hip extension, L_b and L_f change oppositely to the previous case of flexion, as shown in Fig. 2(f). Moreover, the external downward forces can be transmitted to the bony feature of the pelvis through the wire loop and the waist belt. Two dynamic wire loops are symmetrically arranged with respect to the sagittal plane, for the possible application in bilateral knee exoskeletons.

B. Theoretical Analysis

The proposed Dynamic Waist Strap (*C4*) is compared with the three mainstream suspension schemes (*C1*, *C2* and *C3*) theoretically to show its advantages of reducing migration during
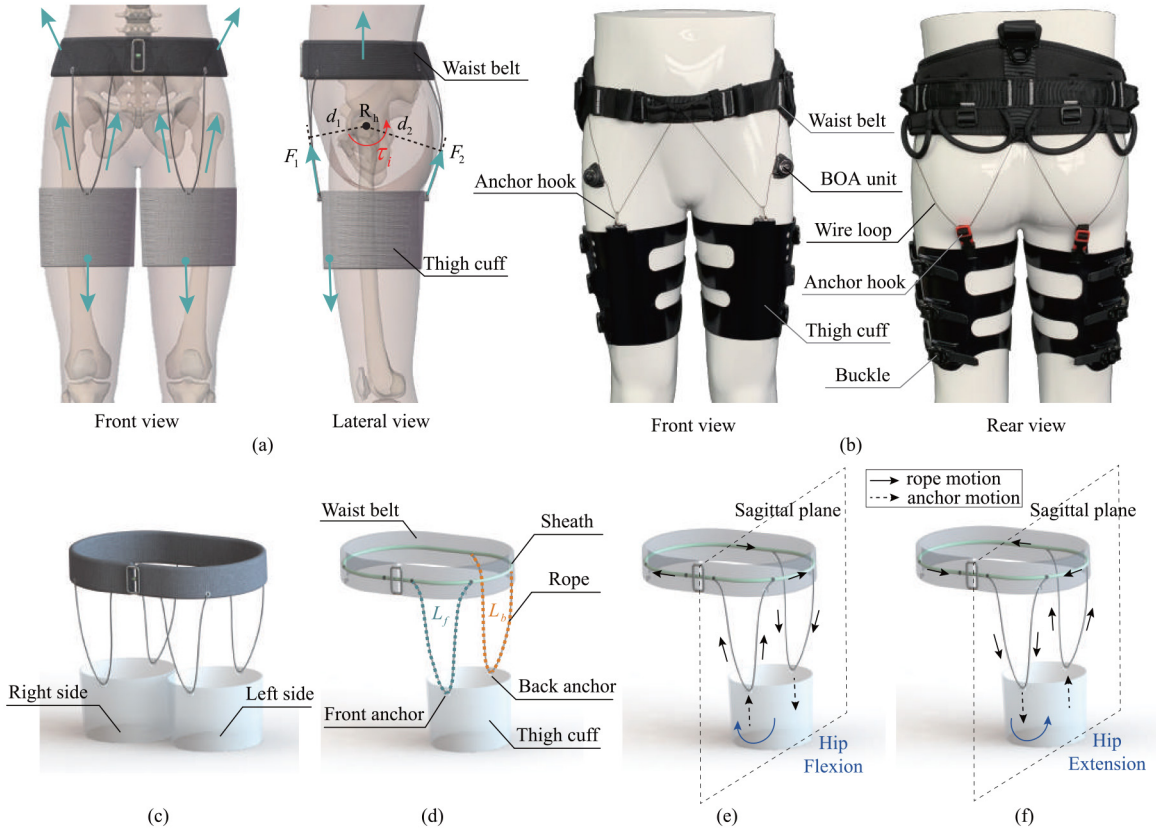
Fig. 2.   The prototype of proposed Dynamic Waist Strap. In (a), R_h is the CoR of the hip joint, the cyan arrows represent the external forces applied to the thigh cuff and the waist belt. Specifically, F_1 and F_2 are the interaction forces between the thigh cuff and the waist belt, d_1, d_2 are the moment arms of F_1 and F_2 relative to R_h, respectively. τ_i is the interaction torque between the suspension system and human, denoted as $\tau_i = F_2 d_2 - F_1 d_1$. In (d), L_f represents the length of the cyan dotted line, and L_b represents the length of the orange dotted line. The black arrows in (e) and (f) visualize the moving direction of the rope and anchors.

hip flexion/extension. To address the mathematical analysis model clearly, several assumptions are made.

- Assumption 1: The deformations of soft tissue in the human thigh, thigh cuff, waist belt, and webbing belts can be neglected.
- Assumption 2: During hip flexion/extension, the thigh cuff only slides along the axis of the human thigh, without any self-rotation.
- Assumption 3: The human thigh shape can be regarded as a cylinder.
- Assumption 4: There is not any friction between the inner surface of the thigh cuff and the skin of the human. During hip flexion/extension, the position of the thigh cuff is determined only by the tightest webbing belt.
- Assumption 5: The geometric relations of human-suspension interaction can be represented by the model in Fig. 3(a), where the human waist thickness, the thigh diameter, the distance between the parallel waistband lower edge and the thigh strap upper edge are equal (set as $2d$) and aligned. The CoR coincides with the geometric center of the thigh cross-section.

It should be noted that these aforementioned assumptions are only used in the theoretical analysis of downward migration, and are not necessary nor reasonable for other indexes. Assumptions 1, 2, and 3 constrain the downward migration to only the movement of the thigh cuff along the human

thigh axis, which are reasonable as the deformation of soft tissue is minor when the human thigh is tightly covered by the thigh cuff, so are the thigh cuff, waist belt, and webbing belts. Assumption 4 is ideal, but it intends to formulate the comparison of different suspension systems in the worst-case scenario, as any friction will help reduce downward migration and result in better results. Assumption 5 represents the human body shape with simple geometric shapes and relations according to the physiological feature of the human body.

Based on the aforementioned assumptions, during hip flexion/extension, the migration of the thigh cuff under the four suspension schemes (*C1-C4*) can be analyzed respectively (see Fig. 3).

1) Lateral Suspension (C1): According to the geometric relations in Fig. 3(b) and applying the cosine theorem in $\Delta R_h W_m T_m'$, we can obtain the distance between the thigh cuff and the CoR of the hip joint (p_1):

$$(2d)^2 = d^2 + p_1{}^2 - 2dp_1 \cos\theta, \tag{1}$$

where

$$\theta = \pi - \alpha. \tag{2}$$

2) Frontal Suspension (C2): During hip flexion, the frontal webbing belt becomes loose and the thigh cuff has the tendency to slide down. In this case, the position of the thigh cuff
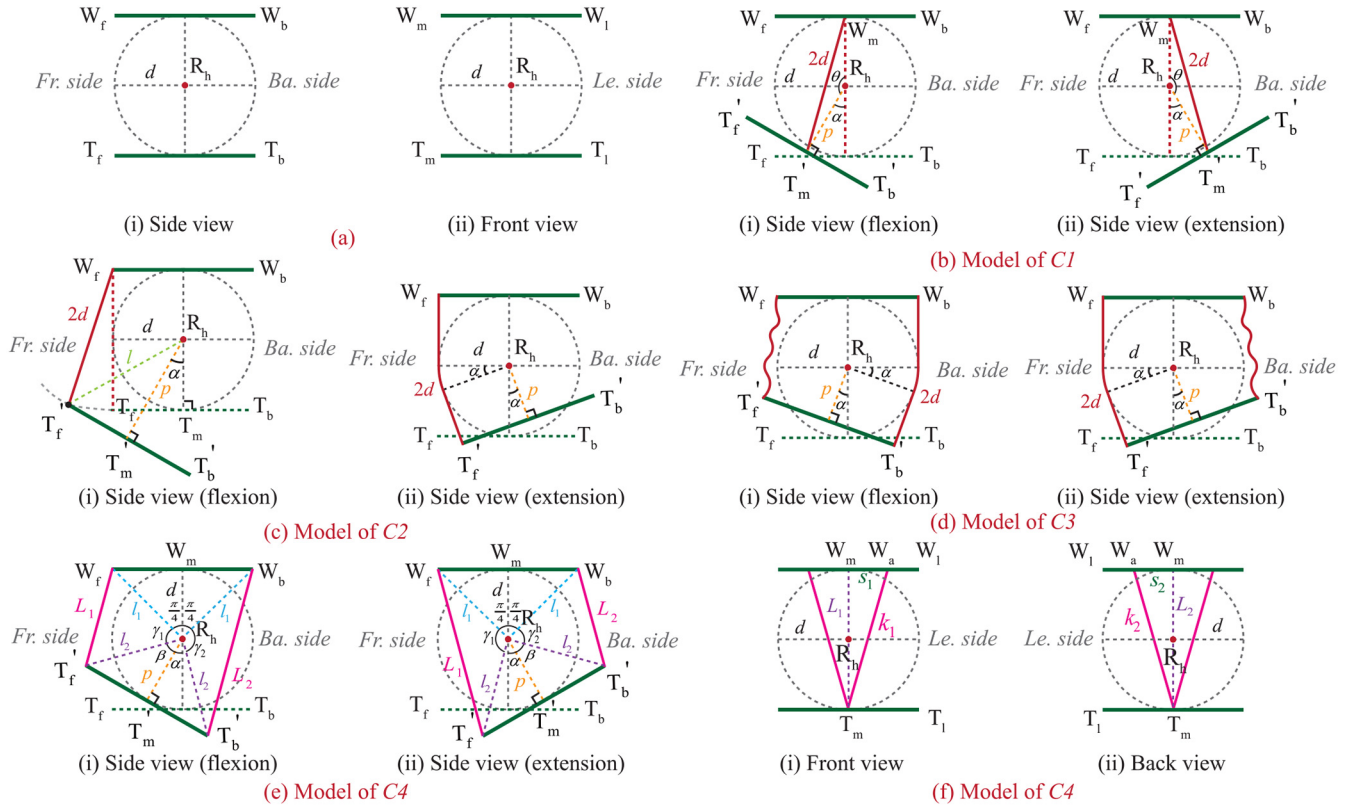
Fig. 3. The sketch map of theoretical analysis for the four different suspension systems. (a) The simplified human-suspension interaction model (includes the hip joint of the human left leg, the thigh cuff of the knee exoskeleton, and the waistband for suspension) is based on the proposed assumptions. (b)-(e) The migration state of the thigh cuff under *C1-C4* (*C1*: the lateral suspension system; *C2*: the frontal suspension system; *C3*: the anterior and posterior suspension system; *C4*: the Dynamic Waist Strap) during hip flexion (left subgraph) or extension (right subgraph). (f) The front (left subgraph) and the back (right subgraph) view when wearing the Dynamic Waist Strap. In this figure, the bold green lines represent the edges of the waistband and the thigh cuff, the bold red lines symbolize the webbing belts utilized for reducing migration, and the bold magenta lines denote the projection of the wire loop embodied in the proposed Dynamic Waist Strap. *Fr* = Front, *Ba* = Back, *Le* = Left. R_h: the CoR of hip joint. W_fW_b: the lower edge of the waistband. T_fT_b: the upper edge of the thigh cuff. α: the angle of the hip joint (zero during normal standing, positive during hip flexion, and negative during hip extension). p: the position of the thigh cuff (the distance between the CoR of the hip joint and the upper edge of the thigh cuff). m: the migrating distance of the thigh cuff (positive when the thigh cuff upwards slides along the thigh axis and negative during downward migration). d is a constant.

is completely determined by the length of the frontal webbing belt (i of Fig. 3(c)).

We can build plane coordinate system with the point R_h as the origin. Then, the equation of the line along the thigh axis is

$$kx_L - y_L = 0, \tag{3}$$

where

$$k = \tan\left(\frac{\pi}{2} - \alpha\right). \tag{4}$$

With constraint of the frontal webbing belt, the point $T_f(x, y)$ is always in circumference, with the point $W_f(-d, d)$ as the center and $2d$ as the radius. Therefore, we can obtain

$$(x + d)^2 + (y - d)^2 = (2d)^2. \tag{5}$$

Moreover, the distance between the point $T_f(x, y)$ and the line along the thigh axis is always d.

$$\left| \frac{kx - y}{\sqrt{k^2 + 1}} \right| = d \tag{6}$$

Since the point $T_f(x, y)$ is always above the line $kx_L - y_L = 0$ during hip flexion, Eq. (6) can be simplified as

$$y = kx + d\sqrt{k^2 + 1}. \tag{7}$$

Besides, according to the geometric relations, the following constraints should be guaranteed:

$$\begin{cases} -3d < x < -d \\ -d < y < 3d. \end{cases} \tag{8}$$

Combined Eq. (4), Eq. (5), Eq. (7) and Eq. (8), we can obtain the coordinate (x, y) of the point T_f when the hip flexes to any angle.

Furthermore, applying the Pythagorean theorem, the distance between the thigh cuff and the CoR of hip joint (p_2) can be calculated through the equations below:

$$\begin{cases} l = \sqrt{x^2 + y^2} \\ p_2 = \sqrt{l^2 - d^2}. \end{cases} \tag{9}$$

During hip extension, the frontal webbing belt is tightened excessively and the thigh cuff tends to upwards slide along the thigh axis. The position of the thigh cuff (p_2) is also completely determined by the length of the frontal webbing belt (ii of Fig. 3(c)).

$$d + \alpha d + p_2 = 2d. \tag{10}$$

3) Anterior and Posterior Suspension (C3): During hip flexion, the anterior webbing belt is slack while the posterior one is tightened excessively. In this case, the thigh cuff migrates upwards along the thigh axis by the pulling of the anterior webbing belt. Similarly, the thigh cuff also slides upwards along the human thigh but is dragged by the posterior webbing belt during hip extension, as shown in Fig. 3(d). The distance between the thigh cuff and the CoR of the hip joint when the hip flexes or extends in *C3* (p_3) is similar to the hip extension process in *C2*, as shown in Eq. (10).

4) Dynamic Waist Strap (C4): As shown in Fig. 3(e), no matter when the hip flexes or extends, the wire loop slides along the sheaths embodied in the waistband to achieve thigh cuff suspension.

Firstly, in $\Delta T_f' T_m' R_h$, the angle β can be expressed as

$$\beta = \arctan\left(\frac{d}{p_4}\right). \tag{11}$$

Secondly, in accordance with the geometric relations illustrated in Fig. 3(e), we can obtain

$$\begin{cases} \gamma_1 = \frac{3}{4}\pi - \alpha - \beta \\ \gamma_2 = \frac{3}{4}\pi + \alpha - \beta. \end{cases} \tag{12}$$

And then, applying the Pythagorean theorem in $\Delta W_f W_m R_h$ and $\Delta T_f' T_m' R_h$, we can obtain

$$\begin{cases} l_1 = \sqrt{2}d \\ l_2 = \sqrt{d^2 + p_4{}^2}. \end{cases} \tag{13}$$

Next, applying the cosine theorem in $\Delta W_f T_f' R_h$ and $\Delta W_b T_b' R_h$, we can obtain

$$\begin{cases} L_1 = \sqrt{l_1^2 + l_2^2 - 2l_1 l_2 \cos \gamma_1} \\ L_2 = \sqrt{l_1^2 + l_2^2 - 2l_1 l_2 \cos \gamma_2}. \end{cases} \tag{14}$$

L_1 in Fig. 3(e) is the projection in the sagittal plane of which is demonstrated in Fig. 3(f), so is L_2. Regardless of any hip rotation state, the length of the wire uncovered by the sheath or the waist belt is changeless, and during normal standing, $L_1 = L_2 = 2d$. Finally, applying the Pythagorean theorem in $\Delta W_a W_m T_m$ of Fig. 3(f), we can obtain

$$\sqrt{L_1^2 + s_1^2} + \sqrt{L_2^2 + s_2^2} = \sqrt{(2d)^2 + s_1^2} + \sqrt{(2d)^2 + s_2^2}. \tag{15}$$

Combined Eq. (11), Eq. (12), Eq. (13), Eq. (14), and Eq. (15), we can obtain the distance between the thigh cuff and the CoR of hip joint (p_4).

Finally, the migrating distance of the thigh cuff (m) under the four suspension conditions can be solved respectively as

$$m = d - p. \tag{16}$$

5) Theoretical Analysis Results: In consideration of actual body size parameters of the common user, a group of initial parameters are chosen for further calculation (unit: cm):

$$\begin{cases} d = 10 \\ s_1 = s_2 = 10. \end{cases} \tag{17}$$

At last, after substituting the initial parameters into the equations in this subsection, the migrating distance of the thigh cuff
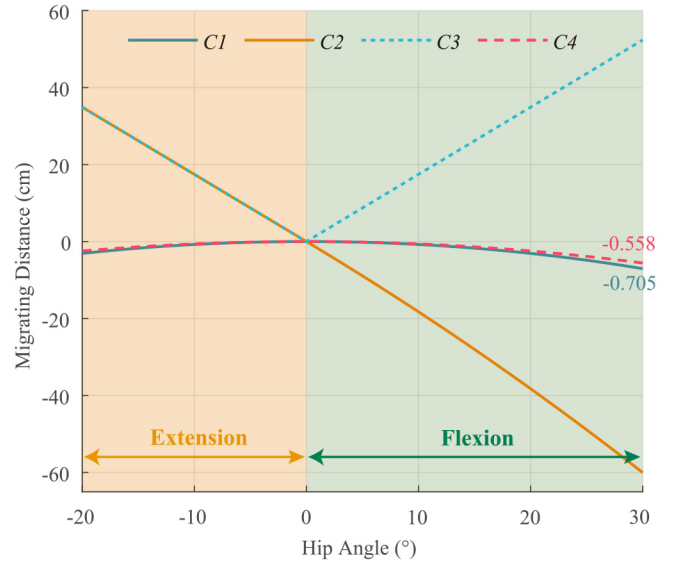

Fig. 4. The theoretical analysis results. The range of hip motion is selected in conformity with the normal walking of healthy people. The migrating distance is positive when the thigh cuff upwards migrates.

under the four different suspension conditions (*C1-C4*) can be calculated and shown in Fig. 4.

It can be seen from Fig. 4 that when the hip flexes range from 0 to 30° or extends from 0 to 20°, the migrating distance of the thigh cuff suspended by the proposed Dynamic Waist Strap (*C4*) is always minimum. Although the theoretical analysis results of *C1* are similar to that of *C4*, the difference between them may be enlarged in experimental validations since the thigh cuff hanged by *C1* has the tendency to rotate relative to the human thigh in the frontal plane. This rotation is not desired for the stability of the thigh cuff but is not considered in the theoretical analysis.

C. Implementation

As illustrated in Fig. 2(b), at last, a prototype design is achieved in accordance with the concept design and the initial parameters for the theoretical analysis described in this section. The prototype consists of a robust waist belt for rock climbing, two wire loops (diameter: 0.8 mm, capacity: 128 lb) arranged symmetrically with respect to the sagittal plane, two corset-like components (BOA Technology Inc., USA), four anchor hooks and several sections of the sheath (diameter: 2.6 mm). The corset-like components are utilized to adjust the initial perimeter of the wire loop, aiming at adapting to the different human figures. Moreover, the corset-like components are also helpful to regulate the pre-tension level of the wire loop, for the purpose of achieving different wearing effects. Besides, the thigh cuff wraps around the human thigh through three buckles, so as to adjust its strapping intensity.

III. MATERIALS AND METHODS

In this section, the development of a testing platform for experimental validations is described, and the protocols of two independent experiments that were carried out are demonstrated. In the first experiment, the effects of four different
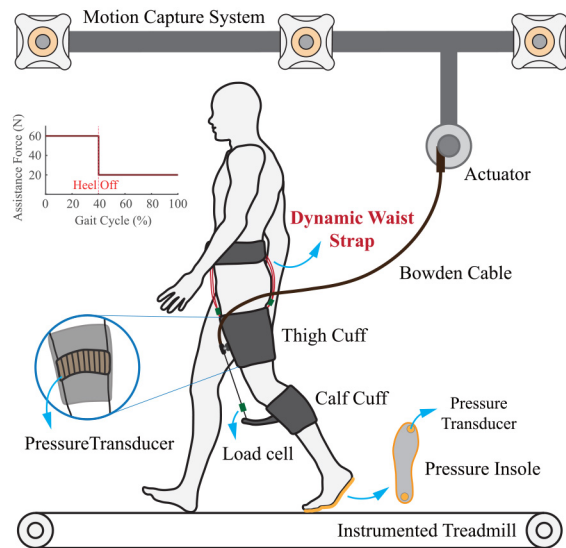
Fig. 5. Overview of the testing platform. The subject is wearing a unilateral knee exosuit on his left leg. The chart in this figure shows the assistance force profile provided by the knee exosuit. The assistance force magnitude appears between the heel strike and the heel off to absorb the impact between the human leg and the ground in the load response phase of the gait cycle. After heel off, the human knee has the tendency to flex, and the effect generated by the soft exosuit is expected to be as transparent as possible, but a cable pre-tension force still exists.

suspension systems (*C1-C4*) on the migrating distance of the thigh cuff, the interaction forces between the suspension system and human, the maximum dip angle of the thigh cuff relative to the human thigh during level-ground walking (with different speeds) are measured. The second experiment is conducted for the further investigation of differences in the migrating distance and the interaction forces when the subjects keep a static posture (hip flexion or extension). The methods used to process the data and evaluate the effects are described in Sections III-C and III-D.

A. Testing Platform

In order to quantify the effectiveness of four different suspension systems (*C1-C4*), a testing platform consists of a soft exosuit for the knee, a twelve-camera reflective marker-based motion capture system, an instrumented treadmill (Gaitway-3D 150/50, h/p/cosmos & Arsalis, Germany & Belgium) and several wearable sensors is developed, as demonstrated in Fig. 5. Since the motion of both sides of the human leg is basically consistent, only a unilateral soft exosuit is utilized in the experiments.

1) Soft Exosuit: The soft exosuit which is powered by a remote actuator can be anchored to the human body via a thigh cuff and a calf cuff, it provides knee extension assistance by retracting a Bowden cable across the front of the knee, which is similar to [16]. When providing extension assistance for the knee, the thigh cuff suffers an external downward pull. For avoiding pressure points, a plastic pad with a form covering its outer surface is arranged between the inner surface of the calf cuff and the human shank, which is helpful to distribute normal forces on either side of the tibial tuberosity. Both cuffs of the soft exosuit (thigh cuff and calf cuff) are designed according

to the surface shape (collected by a three-dimensional scanner) of the subjects' thigh and made of 3D-printed thermoplastic polyurethanes.

2) Actuator: The exosuit is tethered to an off-board actuation system that supplies power, control, and data acquisition. Mechanical power for the exosuit is generated by a brushless DC motor with a 6:1 planetary gearbox, and the motor drives a 43.5 mm radius, single-wrap pulley. The proximal end of the inner wire of Bowden cable is fixed on the pulley, while the distal end of which is anchored to the protrusion on the calf cuff (for the purpose of augmenting the moment arm for knee extension assistance). Moreover, the actuator includes a custom motor driver which tracks a velocity command, a custom magnetic encoder that monitors the kinematic information of the motor, and a custom electronics board with functions of data acquisition and control. The main controller of the actuator runs at 100 Hz, and the control system architecture is based on the hierarchical control framework. Firstly, at the high level, the gait cycle of the human is divided in real-time according to the data collected by the pressure insole. Then, the cable tension planner embodied in the main controller generates the assistance force profile with respect to the gait cycle, and a proportional-integral (PI) controller is applied in force closed-loop control at the middle level. Finally, the motor driver receives the desired velocity value and sends the command to the motor directly. The assistance force profile is illustrated in the chart of Fig. 5. The actuator is capable of being worn on the human body but arranged off-board for the consideration of minimizing the effect of added mass on the subjects.

3) Wearable Sensors: The testing platform employs three miniature single-axis load cells (LSB 205, FUTEK Advanced Sensor Technology Inc., USA) in total, one of them is arranged between two parts of the inner wire of the Bowden cable to achieve force closed-loop control. Other load cells are utilized to measure the interaction force between the thigh cuff and the waist belt (only one is used in *C1* and *C2*). Aiming at adjusting the pre-strapping level of the thigh cuff quantitatively, a 16-channel pressure transducer is used between the cuff and the skin. Besides, a custom pressure insole with 2 pressure transducers at the toe and heel respectively is used to identify the key events (such as heel strike, and heel off) in the gait cycle of the human. Moreover, seven reflective markers are employed in this platform, for kinematic data collection of the wearer and the thigh cuff, as shown in Fig. 6.

B. Experimental Protocol

1) Experimental Design: To describe the effects of different suspension systems (*C1-C4*) on the migrating distance of the thigh cuff and the interaction force(s) between the suspension system and human, two independent trials are conducted in one session. Firstly, a dynamic experiment is conducted for analyzing the effects of suspension systems in level-ground walking with different speeds, 0.7 m/s (low speed), 0.9 m/s (intermediate speed), and 1.1 m/s (high speed) are selected. Secondly, a static posture experiment is conducted for the further investigation of the effects of suspension systems in detail.
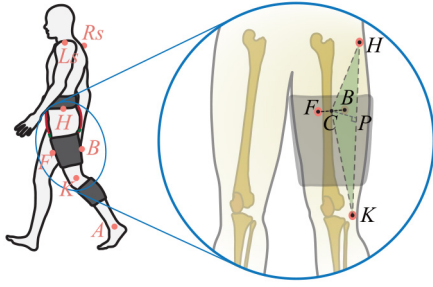
Fig. 6. The arrangement of reflective markers. There are seven reflective markers employed in the experiments in total, the locations of them are demonstrated as the pink points. *Rs*: the right shoulder; *Ls*: the left shoulder; *H*: the hip joint; *K*: the knee joint; *A*: the ankle joint; *F*: the front side of the thigh cuff; *B*: the back side of the thigh cuff. The partially enlarged details illustrate the definition of the thigh cuff's position with respect to the CoR of the hip joint.
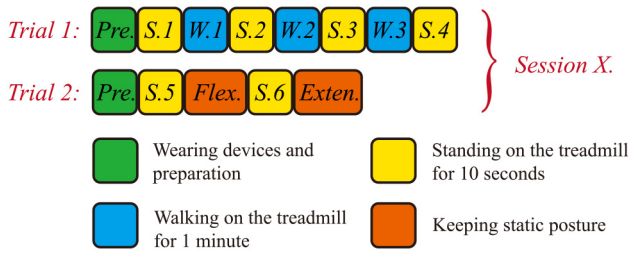

Fig. 7. The experimental process. *Trial 1*: the level-ground walking experiment. *Trial 2*: the static posture experiment. *X* = 1, 2, 3, 4, corresponding to *C1*, *C2*, *C3* and *C4*, respectively. *W.1* = walking with 0.7 m/s; *W.2* = walking with 0.9 m/s; *W.3* = walking with 1.1 m/s.

Before each trial, the thigh cuff of the soft exosuit will be re-worn and adjusted, ensuring it lying right on the uppermost edge of the participants' crotch. Before the experiments, the motion capture system is calibrated, and get the instrumented treadmill is ready for action. The subject stands on the treadmill wearing the soft exosuit, wearable sensors, and a suspension system aforementioned suitably. Then, the hardware communication and data acquisition function of the testing platform is checked, and the pre-tension levels of the thigh cuff and the webbing belt(s) (or the wire loop of *C4*) are adjusted.

Trial 1 (level-ground walking): As Fig. 7 shows, firstly, the participant stands upright on the treadmill for 10 seconds, and the kinematic data of reflective markers collected by the motion capture system and the data collected by the wearable sensors are recorded at this time, for the future calculation of initial conditions (the pre-tension levels and the initial position of the thigh cuff). Then, the subject performs a one-minute walk at the speed of 0.7 m/s, and all the data (reflective markers, force plate, wearable sensors) is recorded in this period. After that, the subject stops moving and stands upright on the treadmill for another 10 seconds with the kinematic data of reflective markers collected for calculating the migrating distance of the thigh cuff, before a one-minute walk with the speed of 0.9 m/s on the treadmill (all the data is recorded). Subsequently, the participant walks at a speed of 1.1 m/s for a minute (all the data is recorded) after standing upright for 10 seconds again (the kinematic data of reflective markers is

collected). The *Trial 1* will be finished after the fourth stance lasting 10 seconds (the kinematic data of reflective markers is collected).

Trial 2 (static posture): As presented in Fig. 7, after the preparation procedure, the subject stands upright on the treadmill for 10 seconds, for the collection of the initial conditions aforementioned. And then, the volunteer flexes his hip joint (left side) to about 30°, and the interaction force(s) between the thigh cuff and the waist belt is recorded to testify to the change of suspension state of the webbing belts. Subsequently, an external downward force is exerted on the thigh cuff through the Bowden cable of the soft exosuit, and the kinematic data of reflective markers are recorded for the future calculation of the migrating distance of the thigh cuff at this time. After that, all the procedures above are repeated except for the subject extending his hip joint to about 20°.

Four sessions of comparative experiments are conducted in total:
- Session 1: subjects wear the lateral suspension system (*C1*, see Fig. 1(a)).
- Session 2: subjects wear the frontal suspension system (*C2*, see Fig. 1(b)).
- Session 3: subjects wear the anterior and posterior suspension system (*C3*, see Fig. 1(c)).
- Session 4: subjects wear the proposed Dynamic Waist Strap (*C4*, see Fig. 1(d)).

2) Subjects: Five healthy subjects (mean ± standard deviation of 22.6 ± 1.36 years old; 72.8 ± 4.58 kg of body mass; 1.75 ± 0.05 m of height) were recruited to participate in the experiments. The study was approved by the local ethics committee of Peking University, and the participants were given informed written consent prior to participation. Three of five participants came to our laboratory for two visits on separate days. The initial visit was to accomplish the *Trial 1* (level-ground walking) of four sessions. When subjects walked at 0.7 m/s on the level treadmill, the magnitude of the assistance force profile was set to 60 N, and 80 N, 100 N for 0.9 m/s and 1.1 m/s respectively. After finishing one trial, the subject took a rest for ten minutes and the suspension system was changed during this period. The second visit was for static posture trials on a separate day. When subjects kept hip flexion or extension posture stably, a constant external downward force (60 N) was exerted on the thigh cuff. Other participants only accomplished the *Trial 1*.

C. Data Acquisition and Processing

The data from the motor driver, motor encoder, load cells, and pressure transducers were synchronously collected and stored by the custom electronics board used to accomplish actuator control and sensor information acquisition with a sampling frequency of 100 Hz. Besides, the raw ground reaction force (GRF) data recorded by the force plate of the instrumented treadmill was collected by an acquisition card (National Instruments, USA), and the captured kinematic data of reflective markers were collected and stored by a personal computer with a sampling frequency of 100 Hz. The raw GRF data was filtered using zero-lag 4th order low pass
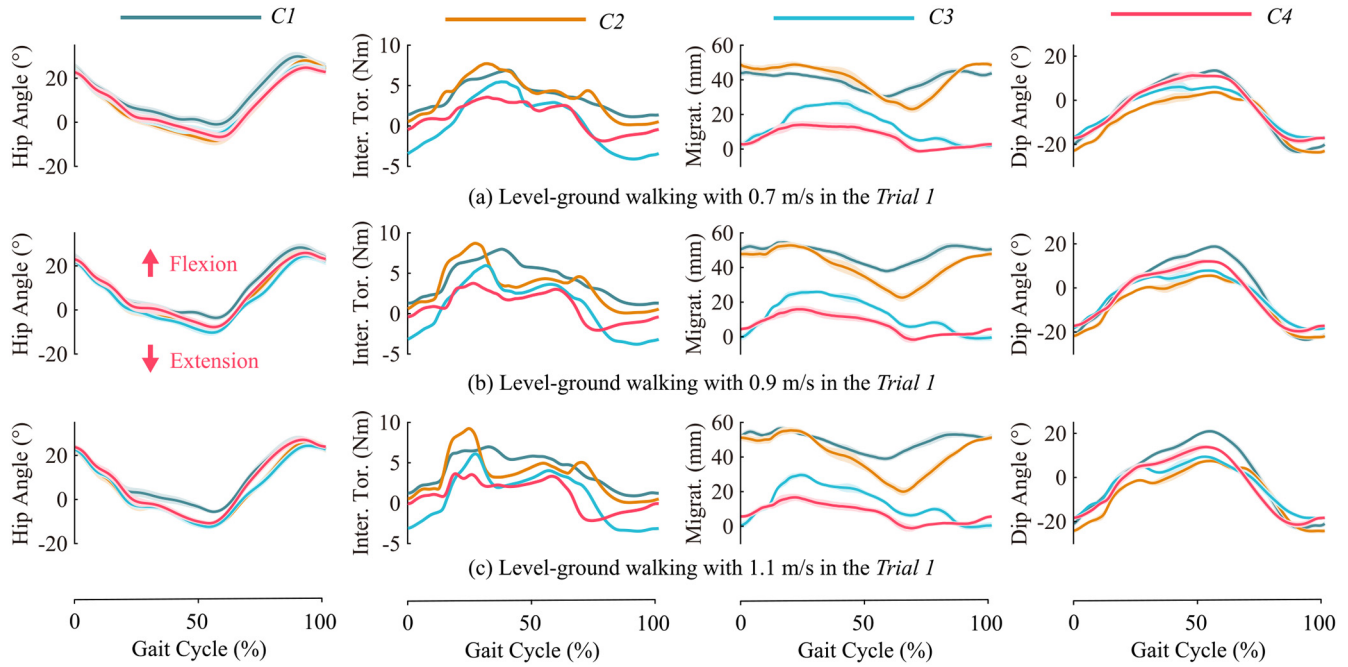
Fig. 8. The dynamic data during level-ground walking from a single subject. The solid lines represent averages across gait cycles, and the shaded areas represent standard deviations. Inter. Tor. is the interaction torque; Migrat. means the migrating distance. In terms of interaction torque, the positive values symbolize hip flexion/abduction torque, while the negative values represent hip extension/adduction torque. In this figure, the dip angle refers to the cuff-to-floor angle.

Butterworth filters with 8 Hz cut-off frequencies. All the data was synchronously collected through a trigger signal.

Furthermore, all the data collected during walking was divided according to the gait cycle of the human detected by the GRF data. In order to ensure that the results were computed from steady-state walking data, the averages were taken from every one-minute walk except the top and the last five gait cycles.

One-way analysis of variance (ANOVA) was used to compare changes among different experimental conditions (in all statistical analyses, the significant level $\alpha = 0.05$), and the least significant difference (LSD) post hoc analysis was performed to determine which differences were significant among conditions.

D. Evaluation Index

1) Migrating Distance: As illustrated in Fig. 6, the point C which indicates the spatial position of the thigh cuff is the midpoint of the line FB, and the line HK describes the axis of the human thigh. In the spatial triangle HKC, the line CP is the perpendicular of the line HK, and the length of line HP represents the position of the thigh cuff relative to the CoR of the hip joint along the thigh axis. Thus, the changes in the line HP's length can be defined as the migrating distance of the thigh cuff.

2) Interaction Torque: It refers to the interaction torque (τ_i) between the suspension system and human, as illustrated in Fig. 2(a). We assume that the directions of the interaction forces captured by load cells (F_1 and F_2) are parallel to each other, and the moment arms of them (d_1 and d_2) are consistent with the initial parameter mentioned in Section II (0.1 m),

during hip flexion/extension. Hence, the interaction torque is the product of the interaction force and the moment arm after vector counteraction, denoted as $\tau_i = 0.1F_2 - 0.1F_1$.

3) Maximum Dip Angle: It refers to the maximum rotation angle of the thigh cuff relative to the human thigh in the sagittal plane. Firstly, we take the cuff-to-floor angle to evaluate it. After subtracting the range of hip angle, the range of cuff-to-floor angle can be defined as the maximum dip angle.

IV. EXPERIMENTAL RESULTS

A. Level-Ground Walking

Before the *Trial 1* of each session, the pre-tension levels of the thigh cuff (strapping force) and the webbing belts (interaction force 1 and 2) were adjusted to the same degree, to guarantee that no significant difference was found among the initial conditions of four sessions. Although the adjustment level was hard to quantify, we tried to ensure that the pre-tension levels of proposed *C4* were no better than others. As illustrated in Fig. 9(a), there was no significant difference among the four experimental conditions in the strapping force of the thigh cuff ($p = 0.933$) and the interaction forces between the thigh cuff and the waist belt ($p = 0.248$, $p = 0.351$ for interaction force 1 and 2, respectively).

1) Migrating Distance: After the *Trial 1* of each session (*S.4*), significant differences were found in the migrating distance of the thigh cuff among the four different suspension systems ($p < 0.001$). Compared with *C1-C3*, utilizing proposed *C4* reduced the migrating distance by $62.00 \pm 22.09\%$ ($p = 0.008$, LSD), $82.17 \pm 7.41\%$ ($p < 0.001$, LSD) and $43.24 \pm 20.34\%$, respectively (Fig. 9(b)). Across five subjects, one-way ANOVA was also applied to test if different
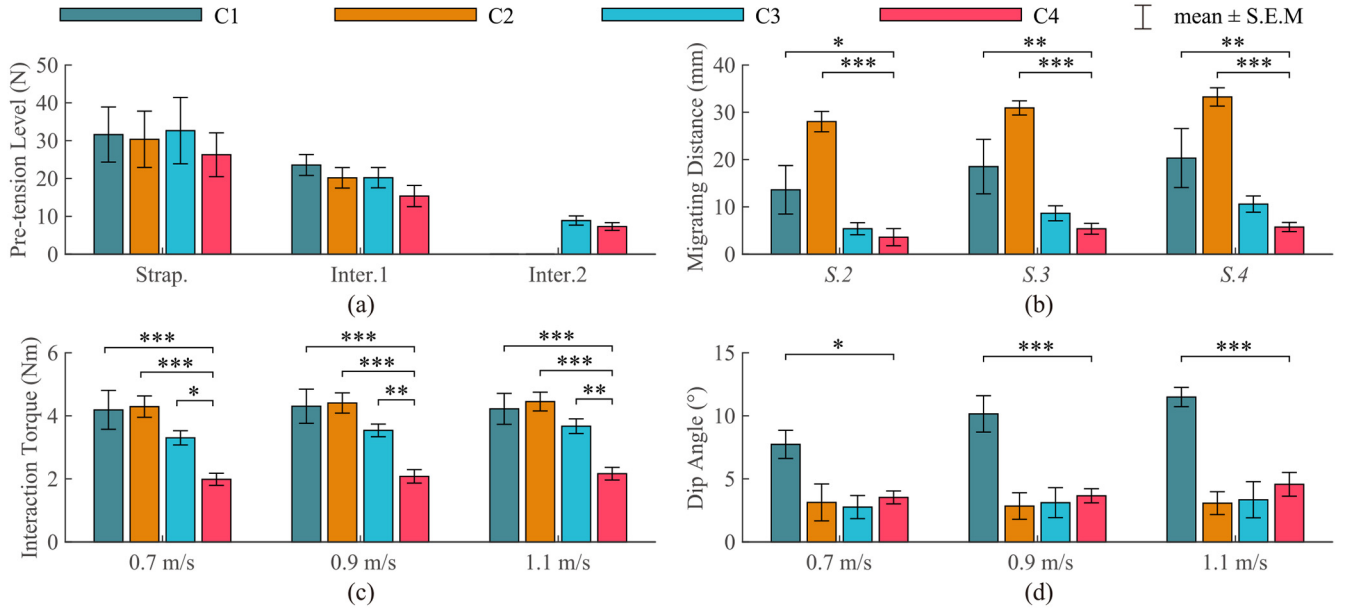
Fig. 9. The statistical results of level-ground walking trials. (a) The initial conditions of four sessions. (b) The migrating distance of the thigh cuff in the *Trial 1*. (c) The average interaction torque across gait cycles between suspension systems and human thigh during level-ground walking in the *Trial 1*. (d) The maximum dip angle of the thigh cuff relative to the human thigh in the sagittal plane during level-ground walking in the *Trial 1*. In this figure, the bars represent the means across five subjects. Strap. is the strapping force; Inter. 1 is the interaction force 1 (collected by the load cell arranged in the anterior or lateral side of the hip joint); Inter. 2 is the interaction force 2 (collected by the load cell arranged in the posterior side of the hip joint); *S.2* is the second stance; *S.3* is the third stance; *S.4* is the fourth stance. *: $p < 0.05$; **: $p < 0.01$; ***: $p < 0.001$.

subjects mattered the migrating distance of the thigh cuff when wearing the same suspension system. The results demonstrated that there was no significant difference across different subjects ($p = 0.811$), which indicated these experimental results were general.

2) Interaction Torque: During level-ground walking with 0.7 m/s (*W.1*), significant differences were found in the average interaction torque between the suspension system and the human thigh across the gait cycle among the four different suspension systems ($p = 0.002$). Compared with *C1-C3*, employing the proposed *C4* reduced the interaction torque by $50.55 \pm 10.33\%$ ($p < 0.001$, LSD), $52.97 \pm 10.22\%$ ($p < 0.001$, LSD) and $39.95 \pm 8.17\%$ ($p = 0.027$, LSD), respectively. During level-ground walking with 0.9 m/s (*W.2*), significant differences were also found ($p < 0.001$). Compared with *C1-C3*, utilizing the proposed *C4* reduced the interaction torque by $50.02 \pm 12.09\%$ ($p < 0.001$, LSD), $52.15 \pm 9.89\%$ ($p < 0.001$, LSD) and $41.14 \pm 9.83\%$ ($p = 0.009$, LSD), respectively. During level-ground walking with 1.1 m/s (*W.3*), significant differences were found in the interaction torque among the four different suspension systems as well ($p < 0.001$). Compared with *C1-C3*, employing the proposed *C4* reduced the interaction torque by $47.00 \pm 12.73\%$ ($p < 0.001$, LSD), $50.80 \pm 9.13\%$ ($p < 0.001$, LSD) and $40.25 \pm 11.81\%$ ($p = 0.005$, LSD), respectively (Fig. 9(c)).

3) Maximum Dip Angle: As shown in Fig. 9(d), the maximum dip angle of the thigh cuff relative to the human thigh differed among the four suspension schemes. The major differences were found between *C1* and *C4*, no matter walking with 0.7 m/s, 0.9 m/s or 1.1 m/s. Compared with *C1*, using *C4* as a hang system could reduce the maximum dip angle of the thigh cuff by $44.25 \pm 40.04\%$ ($p =$
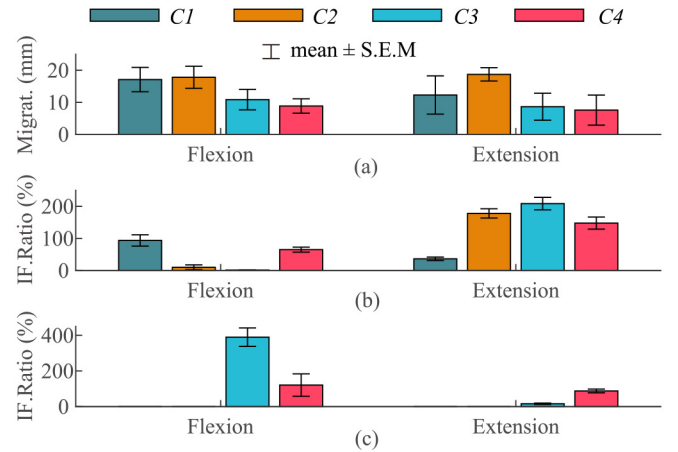

Fig. 10. The statistical results of static posture trials. Migrat. is the migrating distance; IF.Ratio is the interaction force ratio. The bars in this figure represent the averages across three subjects. (a) The migrating distance of the thigh cuff after the hip joint flexed to 30° (or extended to 20°) and a constant external downward force (60 N) was exerted on. (b) The ratio of interaction force 1 (IF.R1) when the hip joint flexed to 30° (or extended to 20°), IF.R1 = (Inter.For.1$_{\text{flex/extend}}$)/(Inter.For.1$_{\text{stance}}$). (c) The ratio of interaction force 2 (IF.R2) when the hip joint flexed to 30° (or extended to 20°), IF.R2 = (Inter.For.2$_{\text{flex/extend}}$)/(Inter.For.2$_{\text{stance}}$).

0.013, LSD, walking with 0.7 m/s), $56.29 \pm 30.24\%$ ($p < 0.001$, LSD, walking with 0.9 m/s) and $60.06 \pm 14.93\%$ ($p < 0.001$, LSD, walking with 1.1 m/s).

B. Static Posture

Before the *Trial 2* of each session, the initial conditions were also adjusted for variable control.

1) Migrating Distance: As described in Fig. 10(a), when the hip flexed and a constant external downward force (60 N)

was applied, the migrating distance of the thigh cuff suspended by *C4* was minimum (8.86 mm), compared with *C1* (17.10 mm), *C2* (17.81 mm) and *C3* (10.85 mm). When the hip extended and a constant external downward force (60 N) was applied, the migrating distance of the thigh cuff suspended by *C4* was minimum as well (7.58 mm), compared with *C1* (12.29 mm), *C2* (18.72 mm) and *C3* (8.64 mm).

2) Interaction Force Ratio: As illustrated in Fig. 10(b), when the hip joint flexed, the interaction force ratio of the frontal webbing belt in *C2* and *C3* decreased sharply to almost zero (1.24% for *C3*), which indicated that the webbing belt is slack in this period. Moreover, when the hip joint extended, the interaction force ratio of the frontal webbing belt in *C2* and *C3* increased substantially (177.96% and 208.56%, respectively), which indicated that the webbing belt suffered from an excessive pull at this time. Fig. 10(c) demonstrated that the interaction force ratio of the posterior webbing belt in *C3* also rose dramatically (389.35%) when the hip joint flexed and fell substantially (15.62%) when the hip joint extended. In contrast, no matter during hip flexion or extension, the interaction force ratios of *C4* were always ranging from 60% to 150%, since the dynamic wire loop of *C4* was tightened properly all the time.

V. DISCUSSION

Downward migration of knee exoskeletons under external forces is one major concern against their normal operations. Several categories of mechanisms have been proposed to address this issue. The high-tighten-able thigh cuffs, including the hook and loop straps [18]–[20], the pneumatic cuffs [6], [21] and the BOA straps [22] do not introduce additional constraints to human joints, but may not be effective under large external downward force, and will cause deformation of human thigh, leading to restraints of muscle activation [23], [24]. The articular ankle/hip joints [25]–[29] introduce extra support against downward migration, but may limit the motion of the corresponding human joint.

The suspension systems attenuate the overwhelming constraints on the human body in comparison to the two previous categories. There are three major types of suspension systems. The lateral suspension system (*C1*) [16] routed an additional webbing strap along the lateral side of the hip. This design is effective in stance, but the webbing strap will be slack during hip flexion, extension, or abduction, leading to unwanted migration of the thigh cuff. Furthermore, if the webbing strap is highly tightened, the thigh cuff may rotate relative to the human thigh in the frontal plane. The frontal suspension system (*C2*) [31]–[33] implements a zonary structure along the anterior side of the hip. The foregoing structure will be slack during hip flexion, yet excessively tightened with hip extension. The anterior and posterior suspension system (*C3*) [34] utilizes two webbing straps arranged along both the anterior and posterior sides of the hip. In this design, if the webbing straps are highly tightened before hip rotation, the thigh cuff of knee exoskeletons can be suspended stably by the waist belt. Nevertheless, this arrangement may hinder the natural motion

of the human hip. If the wearer resists the constraints generated by the webbing straps violently, the connection between the thigh cuff and the waist belt will loosen gradually because of the vibration generated by the user. Therefore, length compensation is necessary for the webbing belts used to achieve knee exoskeleton suspension, since the distance between the waist belt and the thigh cuff changes along with hip rotation, and accomplishing length compensation through deformation is not reliable.

In contrast, this paper proposes a novel suspension system, called the Dynamic Waist Strap (*C4*), which employs wire loops to achieve dynamic length compensation. Both theoretical analysis results demonstrated in Section II and experimental results illustrated in Section IV revealed that the proposed design had obvious advantages in reducing the migration of knee exoskeletons.

In terms of wearing comfort, the proposed Dynamic Waist Strap is expected to provide minimal interaction torque. The experimental results of Section IV indicated that the interaction torque between the suspension system and the human thigh when employing the proposed Dynamic Waist Strap was obviously smaller than in other suspension conditions. Therefore, the wearer will feel more transparent when utilizing the proposed design. Moreover, the maximum dip angle of the thigh cuff when providing suspension is expected to be as small as possible, so that the wearer can be released from the muscle compression by the normal forces from the edges of the thigh cuff. The maximum dip angle of the thigh cuff for the proposed design is much smaller compared with *C1*, and of the same level as *C2* and *C3*, as presented in Section IV.

Furthermore, the proposed design is expected to accommodate different walking speeds so that it can be implemented in daily life. This is experimentally validated by three different walking speeds, as shown in Fig. 9. The statistical analysis results based on the one-way ANOVA also suggest that the effectiveness of the proposed design was not sensitive to different subjects ($p = 0.811$).

The proposed design shows advantageous results regarding downward migration and wearing comfort, in addition to accommodation to variations of walking speed and subject shape with theoretical analysis and/or experiments. It should be admitted that the study still has certain limitations. The theoretical analysis is based on a few assumptions that are valid for downward migration, and the theoretical results match well with experiments. For other indexes, however, these assumptions do not hold anymore, so the theoretical analysis cannot be directly extended. The other limitation is that only five subjects are employed in the study. The results will be statistically stronger with more subjects involved.

Future works of this study may include the following few directions. At first, the location where the wire loop stretches out from the sheath may be adjustable in future design, in order to achieve different wearing effects. Moreover, only level-ground locomotion was included as the dynamic test. Other gaits on different terrains could be included in the future.

VI. Conclusion

In this study, a novel suspension system named the Dynamic Waist Strap was proposed to handle the downward migration of knee exoskeletons through dynamic length compensation. An evaluation system concerning migration and wearing comfort was presented to appraise the effects of suspension systems on the human-exoskeleton system quantitatively. Both theoretical analysis and experimental validations show its effectiveness to reduce downward migration in contrast with the other three existing suspension schemes. Statistical analysis of experimental results also shows its advantages in wearing comfort, in addition to the insensitivity to walking speed and subject shape.

References

[1] T. M. Kepple, K. L. Siegel, and S. J. Stanhope, "Relative contributions of the lower extremity joint moments to forward progression and support during gait," *Gait Posture*, vol. 6, no. 1, pp. 1–8, 1997.

[2] A. M. Dollar and H. Herr, "Lower extremity exoskeletons and active orthoses: Challenges and state-of-the-art," *IEEE Trans. Robot.*, vol. 24, no. 1, pp. 144–158, Feb. 2008.

[3] A. J. Young and D. P. Ferris, "State of the art and future directions for lower limb robotic exoskeletons," *IEEE Trans. Neural Syst. Rehabil. Eng.*, vol. 25, no. 2, pp. 171–182, Feb. 2017.

[4] L. Zhang, G. Liu, B. Han, Z. Wang, H. Li, and Y. Jiao, "Assistive devices of human knee joint: A review," *Robot. Auton. Syst.*, vol. 125, Mar. 2020, Art. no. 103394.

[5] A. T. Asbeck, S. M. De Rossi, I. Galiana, Y. Ding, and C. J. Walsh, "Stronger, smarter, softer: Next-generation wearable robots," *IEEE Robot. Autom. Mag.*, vol. 21, no. 4, pp. 22–33, Dec. 2014.

[6] D. A. Boiten, "The development of a non-migrating knee orthosis," M.S. thesis, Dept. Biomech. Eng., Univ. Twente, Enschede, The Netherlands, 2020.

[7] R. H. Setyabudhy, Z. Liu, and R. P. Hubbard, "Measurement and analysis of human thigh and buttocks contours for aspect manikin development," Technical Paper, SAE, Warrendale, PA, USA, 1999.

[8] R. H. Setyabudhy, A. Ali, R. P. Hubbard, C. Beckett, and R. C. Averill, *Measuring and Modeling of Human Soft Tissue and Seat Interaction*, SAE, Warrendale, PA, USA, 1997.

[9] T. Ishida et al., "Anatomical structure of the subcutaneous tissue on the anterior surface of human thigh," *Okajimas Folia Anatomica Japonica*, vol. 92, no. 1, pp. 1–6, 2015.

[10] D. Zanotto, Y. Akiyama, P. Stegall, and S. K. Agrawal, "Knee joint misalignment in exoskeletons for the lower extremities: Effects on user's gait," *IEEE Trans. Robot.*, vol. 31, no. 4, pp. 978–987, Aug. 2015.

[11] X. Jin, A. Prado, and S. K. Agrawal, "Retraining of human gait-are lightweight cable-driven leg exoskeleton designs effective?" *IEEE Trans. Neural Syst. Rehabil. Eng.*, vol. 26, no. 4, pp. 847–855, Apr. 2018.

[12] K. Langlois et al., "Investigating the effects of strapping pressure on human-robot interface dynamics using a soft robotic cuff," *IEEE Trans. Med. Robot. Bionics*, vol. 3, no. 1, pp. 146–155, Feb. 2021.

[13] K. Langlois, M. Moltedo, T. Bacek, C. Rodriguez-Guerrero, B. Vanderborght, and D. Lefeber, "Design and development of customized physical interfaces to reduce relative motion between the user and a powered ankle foot exoskeleton," in *Proc. 7th IEEE Int. Conf. Biomed. Robot. Biomechatronics (Biorob)*, 2018, pp. 1083–1088.

[14] J. Wang et al., "Comfort-centered design of a lightweight and back-drivable knee exoskeleton," *IEEE Robot. Autom. Lett.*, vol. 3, no. 4, pp. 4265–4272, Oct. 2018.

[15] Z. Zhou, X. Liu, and Q. Wang, "Concept and prototype design of a soft knee exoskeleton with continuum structure (softkex)," in *Proc. Int. Conf. Intell. Robot. Appl.*, 2019, pp. 73–82.

[16] E. J. Park et al., "A hinge-free, non-restrictive, lightweight tethered exosuit for knee extension assistance during walking," *IEEE Trans. Med. Robot. Bionics*, vol. 2, no. 2, pp. 165–175, May 2020.

[17] H. D. Lee, H. Park, B. Seongho, and T. H. Kang, "Development of a soft exosuit system for walking assistance during stair ascent and descent," *Int. J. Control Autom. Syst.*, vol. 18, no. 10, pp. 2678–2686, 2020.

[18] S. Sridar, P. H. Nguyen, M. Zhu, Q. P. Lam, and P. Polygerinos, "Development of a soft-inflatable exosuit for knee rehabilitation," in *Proc. IEEE/RSJ Int. Conf. Intell. Robots Syst. (IROS)*, 2017, pp. 3722–3727.

[19] S. Sridar et al., "Evaluating immediate benefits of assisting knee extension with a soft inflatable exosuit," *IEEE Trans. Med. Robot. Bionics*, vol. 2, no. 2, pp. 216–225, May 2020.

[20] S. Sridar, S. Poddar, Y. Tong, P. Polygerinos, and W. Zhang, "Towards untethered soft pneumatic exosuits using low-volume inflatable actuator composites and a portable pneumatic source," *IEEE Robot. Autom. Lett.*, vol. 5, no. 3, pp. 4062–4069, Jul. 2020.

[21] T. Kermavnar, K. J. O'Sullivan, A. de Eyto, and L. W. O'Sullivan, "Relationship between interface pressures and pneumatic cuff inflation pressure at different assessment sites of the lower limb to aid soft exoskeleton design," *Human Factors*, vol. 63, no. 6, pp. 1061–1075, 2021.

[22] S. V. Sarkisian, M. K. Ishmael, and T. Lenzi, "Self-aligning mechanism improves comfort and performance with a powered knee exoskeleton," *IEEE Trans. Neural Syst. Rehabil. Eng.*, vol. 29, pp. 629–640, Mar. 2021.

[23] T. Kermavnar, K. J. O'Sullivan, V. Casey, A. de Eyto, and L. W. O'Sullivan, "Circumferential tissue compression at the lower limb during walking, and its effect on discomfort, pain and tissue oxygenation: Application to soft exoskeleton design," *Appl. Ergon.*, vol. 86, Jul. 2020, Art. no. 103093.

[24] T. Kermavnar, K. J. O'Sullivan, A. de Eyto, and L. W. O'Sullivan, "Discomfort/pain and tissue oxygenation at the lower limb during circumferential compression: Application to soft exoskeleton design," *Human Factors*, vol. 62, no. 3, pp. 475–488, 2020.

[25] G. G. Pena, L. J. Consoni, W. M. Dos Santos, and A. A. Siqueira, "Feasibility of an optimal EMG-driven adaptive impedance control applied to an active knee orthosis," *Robot. Auton. Syst.*, vol. 112, pp. 98–108, Feb. 2019.

[26] A. C. Villa-Parra et al., "Control of a robotic knee exoskeleton for assistance and rehabilitation based on motion intention from SEMG," *Res. Biomed. Eng.*, vol. 34, no. 3, pp. 198–210, 2018.

[27] J. S. Lora-Millán, J. C. Moreno, and E. Rocon, "Assessment of gait symmetry, torque interaction and muscular response due to the unilateral assistance provided by an active knee orthosis in healthy subjects," in *Proc. 8th IEEE RAS/EMBS Int. Conf. Biomed. Robot. Biomechatronics (BioRob)*, 2020, pp. 229–234.

[28] M. K. Shepherd and E. J. Rouse, "Design and validation of a torque-controllable knee exoskeleton for sit-to-stand assistance," *IEEE/ASME Trans. Mechatronics*, vol. 22, no. 4, pp. 1695–1704, Aug. 2017.

[29] D. Lee, B. J. McLain, I. Kang, and A. J. Young, "Biomechanical comparison of assistance strategies using a bilateral robotic knee exoskeleton," *IEEE Trans. Biomed. Eng.*, vol. 68, no. 9, pp. 2870–2879, Sep. 2021.

[30] M. B. Yandell, B. T. Quinlivan, D. Popov, C. Walsh, and K. E. Zelik, "Physical interface dynamics alter how robotic exosuits augment human movement: Implications for optimizing wearable assistive devices," *J. Neuroeng. Rehabil.*, vol. 14, no. 1, pp. 1–11, 2017.

[31] S. Zhao, Y. Yang, Y. Gao, Z. Zhang, T. Zheng, and Y. Zhu, "Development of a soft knee exosuit with twisted string actuators for stair climbing assistance," in *Proc. IEEE Int. Conf. Robot. Biomimetics (ROBIO)*, 2019, pp. 2541–2546.

[32] K. Schmidt et al., "The myosuit: Bi-articular anti-gravity exosuit that reduces hip extensor activity in sitting transfers," *Frontiers Neurorobot.*, vol. 11, p. 57, Oct. 2017.

[33] F. L. Haufe, K. Schmidt, J. E. Duarte, P. Wolf, R. Riener, and M. Xiloyannis, "Activity-based training with the myosuit: A safety and feasibility study across diverse gait disorders," *J. Neuroeng. Rehabil.*, vol. 17, no. 1, pp. 1–11, 2020.

[34] Y. Zhang, A. Ajoudani, and N. G. Tsagarakis, "Exo-muscle: A semi-rigid assistive device for the knee," *IEEE Robot. Autom. Lett.*, vol. 6, no. 4, pp. 8514–8521, Oct. 2021.

[35] M. Xu, Z. Zhou, J. Shao, and Q. Wang, "Design of a dynamic waist strap for reducing migration of knee exoskeletons," in *Proc. Int. Conf. Intell. Robot. Appl.*, 2021, pp. 687–697.